(Fig. 1). The first nonsense mutation is a homozygous [G92A] mutation in families DUK 1404 and DUK 1405, confirming the shared haplotype over this region. The single–base pair mutation in the first exon converts a codon specifying tryptophan (amino acid 31) to a nonsense codon and is predicted to result in a truncated protein. Family DUK 1402 has a second homozygous nonsense mutation in exon 5 [C581G], which converts a codon specifying serine (amino acid 194) to a nonsense codon and is also predicted to result in a truncated protein. This family does not share any haplotype with the other families over the entire CMT4A region.

The third mutation is a missense mutation in DUK 1403. This is a homozygous [G482A] mutation in exon 3 that causes a [R161H] change. Although this is a conservative amino-acid change, the 204 control chromosomes tested did not show the base-pair change (for sequence tracings and molecular methods, see Web Figs B and C and Web Note A) .

The observation of three different mutations in these four geographically and ethnically close Tunisian families was unexpected. We do not know whether these mutations are attributable to chance, to a region with a high mutation rate or to a frequent gene defect.

Little is known about the function of *GDAP1*. It gives rise to a 4.1-kb transcript and encodes 358 amino acids. The mouse and human proteins have 94% homology. The carboxy-terminal region contains a glutathione S transferase (GST) domain, along with two or three transmembrane helices. Liu *et al.*[5] used α-2, 8-sialyltransferase (GD3 synthase) activation to initiate cholinergic differentiation with neurite sprouting in a Neuro2a neuroblastoma cell line. *GDAP1* was highly expressed during this activation. It seems to be developmentally regulated in mouse brain, with maximal expression in adult brains, and was found to be specifically expressed in neural tissue. Notably, *GDAP1* is expressed in both Schwann cells, the primary source of cDNA in the cauda equina, and the central nervous system. This suggests that *GDAP1* may have a role in the nervous system other than its involvement in cell differentiation, the disruption of which leads to CMT4A.

A new locus was recently reported[6] for autosomal recessive axonal CMT in Tunisian families, between markers *D8S1807* and *D8S548*. This region overlaps *GDAP1* and raises the question of whether mutations in *GDAP1* can cause both axonal and demyelinating neuropathic phenotypes. The answer is yes: on page 22, Cuesta *et al.*[7] report that Spanish families with axonal neuropathy families do have *GDAP1* mutations. This finding supports reports that a known CMT1 gene, *MPZ* (P_0) can also cause axonal (CMT2) phenotypes[3]. The finding of *GDAP1* mutations in these two reports shows that this axonal and demyelinating delineation[8,9], although useful, does not imply unique etiologies.

Our finding that mutations in *GDAP1* lead to CMT4A suggests a potentially unique mechanism leading to this demyelinating neuropathy. This work should continue to provide insight into the normal and disease mechanisms of peripheral nerve biology.

Note: Supplementary information is available on the Nature Genetics web site (http://genetics.nature.com/supplementary_info/).

Acknowledgments

This work was supported by grants from the National Institutes of Health. We would like to thank S. Stinnett at GlaxoSmithKline, RTP, for technical assistance in helping construct the shotgun sequence.

Rachel V. Baxter[1], Kamel Ben Othmane[1], Julie M. Rochelle[1], Jason E. Stajich[1], Christine Hulette[1], Susan Dew-Knight[1], Faycal Hentati[2], Mongi Ben Hamida[2], S. Bel[2], Judy E. Stenger[1], John R. Gilbert[1], Margaret A. Pericak-Vance[1] & Jeffery M. Vance[1]

[1]Center for Human Genetics, Institute of Genomic Sciences and Policy, Research Park Building II Room 105, Box 2903, Duke University Medical Center, Durham, North Carolina 27710, USA. [2]Institut National de Neurologie, La Rabta, 1007 Tunis, Tunisia. Correspondence should be addressed to J.M.V. (e-mail: jeff@chg.mc.duke.edu).

Received 23 July; accepted 12 November 2001

1. De Jonghe, P., Timmerman, V., Nelis, E., Martin, J.J. & Van Broeckhoven, C. *J. Peripher. Nerv. Syst.* **2**, 370–387 (1997).
2. Ben Othmane, K. *et al. Hum. Mol. Genet* **2**, 1625–1628 (1993).
3. Vance, J.M. The many faces of Charcot-Marie-Tooth disease. *Arch. Neurol.* **57**, 638–640 (2000).
4. Ben Othmane, K. *et al. Neurogenetics* **18**, 18–23 (1998).
5. Martinotti, A. *et al. Hum. Mol. Genet.* **1**, 331–334 (1992).
6. Barhoumi, C. *et al. Neuromuscul. Disord.* **11**, 27–34 (2001).
7. Cuesta, A. *et al. Nature Genet.* **30**, 22–25 (2001).
8. Dyck, P.J. & Lambert, E.H. *Arch. Neurol.* **18**, 603–618 (1968).
9. Dyck, P.J. & Lambert, E.H. *Arch. Neurol.* **18**, 619–625 (1968).

The gene encoding ganglioside-induced differentiation-associated protein 1 is mutated in axonal Charcot-Marie-Tooth type 4A disease

Published online: 17 December 2001, DOI: 10.1038/ng798

We identified three distinct mutations and six mutant alleles in *GDAP1* in three families with axonal Charcot-Marie-Tooth (CMT) neuropathy and vocal cord paresis, which were previously linked to the CMT4A locus on chromosome 8q21.1. These results establish the molecular etiology of CMT4A (MIM 214400) and suggest that it may be associated with both axonal and demyelinating phenotypes.

Charcot-Marie-Tooth disease is the most frequently occurring inherited peripheral neuropathy. CMT is classified in two main groups[1,2]: (i) demyelinating CMT, associated with reduced nerve conduction velocities and segmental de- and remyelination and onion bulb formations, and (ii) axonal CMT, characterized by axonal degeneration without demyelinating lesions and the presence of clusters of regeneration. We diagnosed an axonal CMT phenotype associated with hoarse voice and vocal cord paresis in two small families, LF20 and LF249, and one large inbred family, LF38, with Spanish ancestry. The disease segregates as an autosomal recessive trait. The clinical picture is characterized by onset at childhood with weakness and foot and hand wasting, leading to disability at the end of the first decade[3]. Sensory-nerve action potentials were decreased or absent in all affected individuals. In families LF20 and LF249, we did not register median, ulnar, and peroneal compound motor action potentials (CMAPs). However, we obtained

CMAPs in axillaris nerves with distal latencies within the normal range (3.7 ms and 3.2 ms, respectively; the normal limit is <5.3 ms). In family LF38, motor-nerve conduction velocities in distal median and ulnar nerves were slightly reduced (41 m s^{-1}, with a CMAP of 1.4 mV, and 42 m s^{-1}, with CMAP of 0.8 mV, respectively) and were normal in proximal median nerves (58 m s^{-1}). Notably, sural nerve biopsies of two probands showed loss of myelinated fibers and axonal degeneration, with no signs of demyelination and remyelination.

We obtained cumulative lod scores of 6.2 and 4.6 at θ=0.00 with STR markers *D8S286* and *D8S164*, respectively (Web Table A), originally associated with the CMT4A locus, suggesting that the candidate gene mapped to chromosome 8q21.1 (refs 4–6). We further analyzed the large inbred family for ancestral recombination events by homozygosity mapping (Fig. 1)[7]. Loss of homozygosity was observed distal to marker *D8S541* in patient V.1 and proximal to marker *D8S551* in patients IV.12 and IV.14, placing the gene within the 2-cM interval flanked by these two markers.

The gene *GDAP1* (ref. 8) maps within the genetic candidate region. The homolog *Gdap1* is highly expressed in mouse brain and was identified after ganglioside-induced differentiation of the mouse neuroblastoma cell line Neuro2a[8]. This gene may be involved in a signal transduction pathway in neuronal development. *GDAP1* spans 13.9 kb of genomic DNA, with the coding sequences split into 6 exons. The sequence of *GDAP1* contains an ORF of 1,077 nt and encodes a 358-aa protein[8]. A 2,505-bp EST (AL110252) located 344 nt downstream of the stop codon of *GDAP1*, shows two putative polyadenylation signals. We postulated that this sequence may be part of *GDAP1* (Fig. 2*a*). We amplified a 754-bp product from total brain cDNA using nested primers based on the *GDAP1* exon 6 and AL110252 sequences (Fig. 2*b*), suggesting that the EST is an untranslated part of exon 6.

Northern-blot analysis showed the greatest *GDAP1* expression in whole brain and spinal cord. We identified a 3.9-kb major transcript, in agreement with the size predicted from the AL110252-containing mRNA (Fig. 2*c*). We confirmed, by RT–PCR, ubiquitous expression in several human (Fig. 2*d*) and mouse tissues (Fig. 2*e*), with apparently predominant expression in nervous system tissues. Amplification of human sural nerve and mouse sciatic nerve transcripts suggests that *GADP1* expression does not occur just in neurons but also in Schwann cells. When expression levels of different nervous tissues are compared, however, *GDAP1* expression is higher in central tissues than in peripheral nerves.

We PCR-amplified and directly sequenced the entire coding region of *GDAP1*, including exon–intron boundaries, in probands of the three families with CMT (Web Table B). We identified (i) six mutant alleles and three distinct mutations; (ii) two nucleotide substitutions; (iii) a C487T transition in exon 4 and a C581G transversion in exon 5 that generate two nonsense mutations, Q163X and S194X, respectively; and (iv) insertion 863insA in exon 6, leading to a frameshift mutation that generates two abnormal amino acids after threonine 288 and terminates the protein at codon 290 (T288fsX290). Family LF38 proband (IV:1) was homoallelic for the Q163X mutation (Fig. 2*f*). Using *Hae*III restriction analysis, we observed complete segregation between the mutation and the disease (Fig. 2*g*). The proband from family LF249 was a compound heterozygote with respect to Q163X and S194X mutations (Fig. 2*f*). The index individual from family LF20 was heteroallelic with respect to Q163X and T288fsX290 (Fig. 2*f*). We confirmed mendelian segregation of the disease in these two families by *Hae*III restriction analysis, SSCP analysis and ASO analysis (data not shown). These nucleotide changes were not observed in 134 normal chromosomes.

The amino-acid sequence of GDAP1 shows strong similarity to glutathione S-transferases (GSTs), enzymes that have a role in the detoxification of cells. By secondary structure analysis we detected the $\beta\alpha\beta\alpha\beta\beta\alpha$ topology of the glutathione (GSH) binding site of the N-terminal thioredoxin-like fold domain of GSTs in

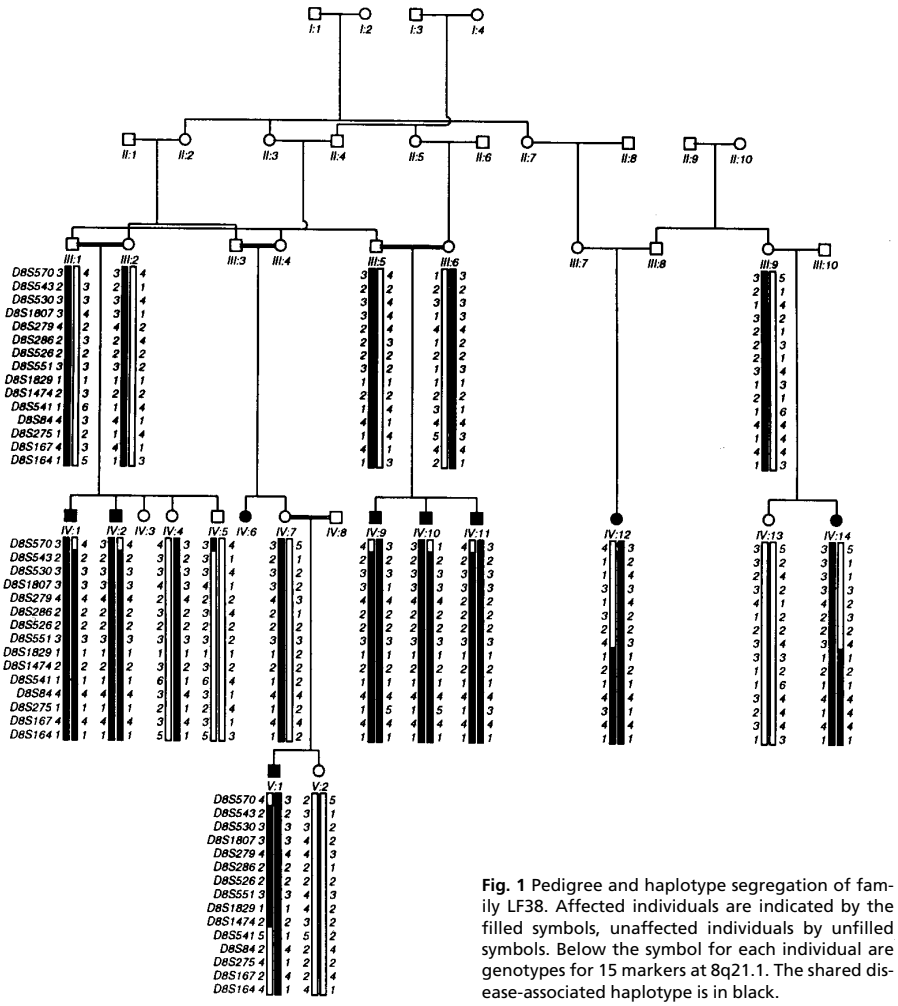

Fig. 1 Pedigree and haplotype segregation of family LF38. Affected individuals are indicated by the filled symbols, unaffected individuals by unfilled symbols. Below the symbol for each individual are genotypes for 15 markers at 8q21.1. The shared disease-associated haplotype is in black.

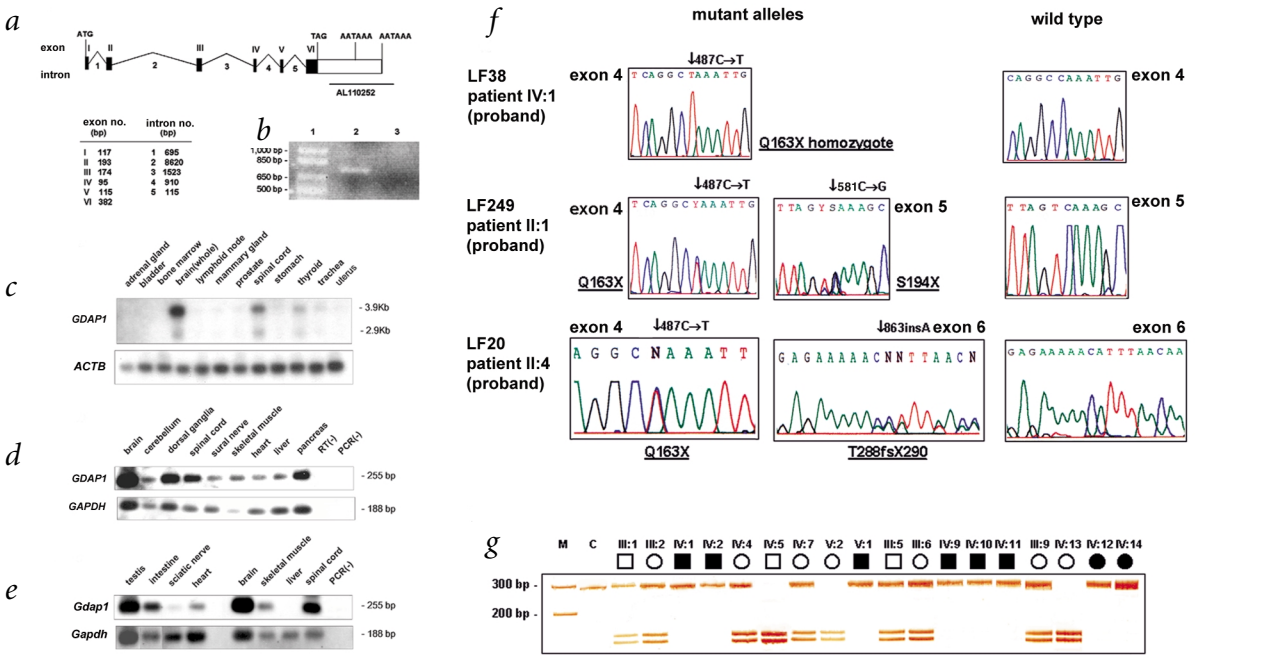

Fig. 2 Molecular analysis of *GDAP1*. ***a***, Diagram showing exon–intron structure. Exons are indicated by black boxes; exon 6 coding sequence is in black and the noncoding sequence is in white. The position of AL110252 EST is indicated as a solid bar. ***b***, Nested PCR between exon 6 and AL110252 (lane 2). ***c***, Northern-blot analysis with a 1,015-bp cDNA probe shows both the major 3.9-kb transcript and a minor 2.9-kb transcript that are more abundant in brain (whole), spinal cord and thyroid gland. β-actin gene *ACTB* was used as an internal control for the amount of RNA in each sample. ***d***,***e***, RT–PCR analysis of *GDAP1* and *GAPDH* (control) transcripts in human (*d*) and mouse (e) tissues. RT(–), no reverse transcriptase was added to the first-strand reaction of the brain RNA. PCR(–), no first-strand template was added to the PCR reaction. ***f***, Direct sequences of *GDAP1* mutations identified in the three probands. Mutation changes for exons 4, 5 and 6 are represented on the left side and normal controls are shown on the right. ***g***, Segregation of the Q163X mutation in family LF38 revealed by restriction analysis. PCR amplification product of wildtype DNA produces a 288-bp band. A C487T substitution destroys an *Hae*III restriction site that normally generates two fragments of 148 and 140 bp in the wildtype. Affected individuals (filled boxes or circles) show a unique undigested band of 288 bp, indicating that they are homozygous with respect to the Q163X mutation. Obligate carrier parents and carrier sibs show one undigested 288-bp band and the two digested 148- and 140-bp bands. Noncarrier individuals only show the two digested fragments. M, 1-kb plus DNA ladder weight marker. C, undigested control PCR product.

amino-acid residues 26–119, followed by the detection of an α-helical domain II for recognition of xenobiotic substrates[9–11]. By analyzing the secondary structure, we detected the two domains of GSTs. Amino-acid residues 26–119 show the βαβαββα topology of the glutathione (GSH) binding site, and amino-acid residues 210–287 show the α-helical domain II that may recognize xenobiotic substrates[9–11]. The carboxy-terminal sequence of GDAP1 has two putative transmembrane domains. Phylogenetic analyses showed that GDAP1 belongs to a newly discovered and probably monophyletic group of GSTs that includes the mouse protein and others from *Drosophila melanogaster*, CG4623, and *Arabidopsis thaliana*, T14N5.14.

In this issue, Baxter *et al.* have also identified mutations in *GDAP1* in the Tunisian families with CMT4A[12] described as a severe demyelinating neuropathy of childhood[4,13]. Genetic data confirm that mutations in *GDAP1* may be associated with both axonal and demyelinating phenotypes, as reported for other inherited peripheral neuropathies[14]. We suggest a putative role for GDAP1 in the interaction between Schwann cell and axon that, when interrupted, may cause either axonal degeneration or demyelination in peripheral nerve. Mutated *GDAP1* might prevent the correct catalyzing S-conjugation of reduced GSH, resulting in progressive attrition of both axons and Schwann cells.

GenBank accession numbers. *GDAP1* cDNA, Y17849; GDAP1 protein, CAA76892.

NCBI reference sequences (RefSeq) for *GDAP1*. Genome contig, NT_008209; model nucleotide, XM_005273; model protein, XP_005273.

Note: Supplementary information is available on the Nature Genetics web site (http://genetics.nature.com/supplementary_info/).

Acknowledgments

We thank the members of the three families for their collaboration. We also thank G. López-Carballo and D. Barettino for help with northern blot experiments, A. Díez-Juan for preparing mouse tissues, J. Carmona for collaboration in the artwork design and P. González-Cabo and R. Vázquez-Manrique for discussions. A.C. is the recipient of a predoctoral fellowship from the Instituto de Salud Carlos III, and L.P. is the recipient of a fellowship from the Fundació Karl Faust, Estació Internacional de Biologia Mediterrànea, and a predoctoral fellowship from the Spanish Ministry of Science and Technology. This work was supported by grants from the Comisión Interministerial de Ciencia y Tecnología and the Fondo de Investigación Sanitaria. E.L. and F.P. are members of the European CMT Consortium (Biomed 2 concerted action CT961614).

Ana Cuesta[1], Laia Pedrola[1], Teresa Sevilla[2], Javier García-Planells[1], María José Chumillas[3], Fernando Mayordomo[4], Eric LeGuern[5,6], Ignacio Marín[7,8], Juan J. Vílchez[2] & Francesc Palau[1,7]

[1]Laboratory of Genetics and Molecular Medicine, Instituto de Biomedicina, Consejo Superior de Investigaciones Científicas (CSIC), 46010 Valencia, Spain. Departments of [2]Neurology, [3]Clinical Neurophysiology and [4]Pathology, Hospital Universitari La Fe, Valencia, Spain. [5]INSERM U289 and [6]Departement de Génétique, Cytogénétique et Foetopathologie, Hôpital Pitié-Salpêtrière, Paris, France. [7]Department of Genetics and [8]Institut Cavanilles de Biodiversitat i Biologia Evolutiva, Universitat de València, Burjassot, Valencia, Spain. Correspondence should be addressed to F.P. (e-mail: fpalau@ibv.csic.es).

Received 2 August; accepted 19 November 2001.

1. Dyck, P.J., Chance, P., Lebo, R. & Camey, J.A. in *Peripheral Neuropathy* (eds Dyck, P.J., Thomas, P.K., Griffin, J.W., Low, P.A. & Poduslo, J.F) 1094–1136 (W B Saunders, Philadelphia, 1993).
2. Lupski, J.R. & Garcia, C.A. in *The Metabolic and Molecular Bases of Inherited Disease* (eds Scriver, C.R. *et al.*) 5759–5788 (McGraw-Hill, New York, 2001).
3. Sevilla, T. *et al. Acta Myol.* **20**, 49–52 (2001).
4. Ben Othmane, K. *et al. Hum. Mol. Genet.* **2**, 1625–1628 (1993).
5. Ben Othmane, K. *et al. Genomics* **28**, 286–290 (1995).
6. Ben Othmane, K. *et al. Neurogenetics* **2**, 18–23 (1998).
7. Lander, E.S. & Botstein, D. *Science* **236**, 1567–1570 (1987).
8. Liu, H., Nakagawa, T., Kanematsu, T., Uchida, T. & Tsuji, S. *J. Neurochem.* **72**, 1781–1790 (1999).
9. Salinas, A.E. & Wong, M.G. *Curr. Med. Chem.* **6**, 279–309 (1999).
10. Hayes, J.D. & Pulford, D.J. *Crit. Rev. Biochem. Mol. Biol.* **30**, 445–600 (1995).
11. Armstrong, R.N. *Chem. Res. Toxicol.* **10**, 2–18 (1997).
12. Baxter, R.V. *et al. Nature Genet.* **30**, 21–22 (2001).
13. Hentati, F. *et al. Acta Myol.* **20**, 25–28 (2001).
14. Lewis, R.A., Sumner, A.J. & Shy, M.E. *Muscle Nerve* **23**, 1472–1487 (2000).

Small changes in expression affect predisposition to tumorigenesis

Published online: 17 December 2001, DOI: 10.1038/ng799

We have used quantitative measures of gene expression to show that constitutional 50% decreases in expression of one adenomatous polyposis coli tumor suppressor gene (*APC*) allele can lead to the development of familial adenomatous polyposis.

Much of the phenotypic variation among closely related organisms is due to changes in gene expression rather than to alterations in protein sequence[1]. Consequently, it might be expected that variations in disease phenotype would frequently be caused by changes in expression levels rather than structural alterations of genes. However, few examples of genes in which small changes in expression result in severe disease have been documented[2]. Here we show that slightly lower levels of *APC* expression are associated with a pronounced predisposition to hereditary colorectal tumors.

Notably, in a study designed to detect the causative mutations in individuals with familial adenomatous polyposis (FAP)[3], tentative evidence was obtained[4] for a partial reduction in APC protein expression in one affected person (patient 1). To search for sequence variations in the coding region of *APC* that might explain this reduction, we isolated the alleles of patient 1 using Conversion technology[5]; however, no sequence variations, other than previously described polymorphisms, were identified in either allele.

To determine whether a reduction in mRNA levels might account for the reduced protein levels, we quantified the relative levels of mRNA transcripts from each *APC* allele using Digital-SNP[6]. This technique involves dilution of template (genomic DNA in past studies, reverse-transcribed cDNA in this study) so that there is on average less than one template molecule per well in a multi-well plate. PCR products are scored with fluorescent probes that discriminate between the two alleles, and the data is rigorously analyzed using likelihood methods[6].

Using Digital-SNP, genomic DNA from the proband yielded the expected 50% allelic ratio, but cDNA from lymphoblastoid cells showed a skewed distribution, with a ratio of approximately 66% (Fig. 1). Linkage analyses with this SNP showed that the allele whose mRNA was expressed in lower relative amounts was the one linked to disease (lod score of 3.84 at recombination fraction θ of zero). Lymphoblastoid-derived RNA from four other affected members of the kindred each had allele ratios of approximately 66% in cDNA, with the linked allele always expressed less, whereas the cDNA from lymphoblastoid cells of 24 unrelated individuals without FAP showed normal allele ratios (Fig. 1).

We found additional evidence for the pathogenic significance of this allele by studying loss of heterozygosity (LOH) of *APC* in benign tumors from this kindred. DNA from the non-neoplastic fractions of these tumors had balanced (50%) allelic ratios, whereas DNA from the neoplastic fractions of 23 of 28 tumors had allelic loss (Fig. 2). In 22 of the 23 tumors showing LOH, the allele lost in the tumors was the normal allele—that is, the one that was expressed at relatively higher levels and not linked to disease ($P<0.0001$).

To determine whether similar small decreases in expression could be observed in other individuals with FAP, we examined four people with FAP who had no *APC* abnormalities evident upon IVSP or sequencing of Conversion-separated alleles. One (patient 2) of these four affected individuals had an abnormal, 71% allelic ratio of alleles in cDNA (Fig. 1). No affected relatives were available

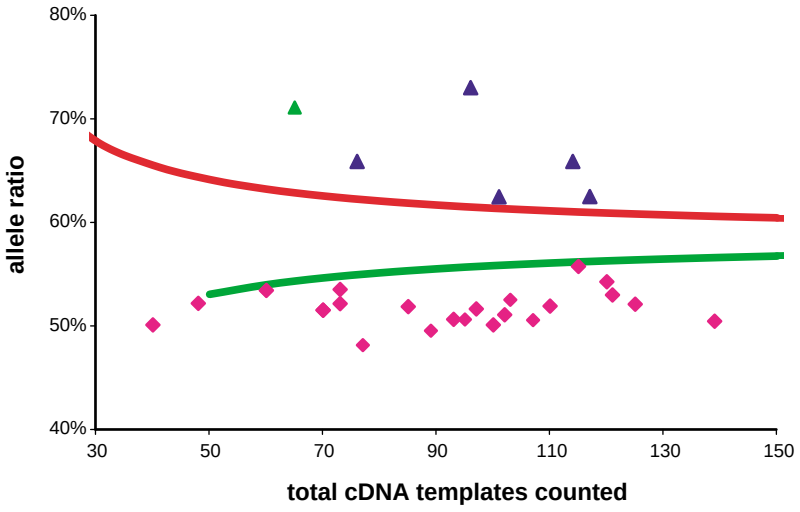

Fig. 1 Reduced expression of one allele in affected individuals with FAP. Dig-SNP analysis of cDNA was carried out to quantify the relative levels of transcription products of the two *APC* alleles. The SNPs used for these analyses were at *APC* codons 486 or 1756 (ref. 9). The five blue triangles represent patient 1 and four of his affected relatives, the green triangle represents patient 2 and the pink diamonds represent controls that did not have FAP. Points above the red curve provide strong evidence that one allele is expressed at lower levels than the other[6,10].